

Article

Monitoring and Analysing Land Use/Cover Changes in an Arid Region Based on Multi-Satellite Data: The Kashgar Region, Northwest China

Ayisulitan Maimaitiaili ^{1,*}, Xiaokaiti Aji ², Akbar Matniyaz ¹ and Akihiko Kondoh ³

¹ Geosystem and Biological Sciences Division, Graduate School of Science, Chiba University, Chiba 263-8522, Japan; akbar120311@gmail.com

² Pacific Consultants Co., Ltd., Chiyoda 101-8462, Japan; kaiti1103@gmail.com

³ Center environmental remote sensing, Chiba University, Chiba 263-8522, Japan; kondoh@faculty.chiba-u.jp

* Correspondence: Aysultan@chiba-u.jp

Received: 3 November 2017; Accepted: 9 January 2018; Published: 12 January 2018

Abstract: In arid regions, oases ecosystems are fragile and sensitive to climate change, and water is the major limiting factor for environmental and socio-economic developments. Understanding the drivers of land use/cover change (LUCC) in arid regions is important for the development of management strategies to improve or prevent environmental deterioration and loss of natural resources. The Kashgar Region is the key research area in this study; it is a typical mountain-alluvial plain-oasis-desert ecosystem in an arid region, and is one of the largest oases in Xinjiang Uyghur Autonomous Region, China. In addition, the Kashgar Region is an important cotton and grain production area. This study's main objectives are to quantify predominant LUCCs and identify their driving forces, based on the integration of multiple remote sensors and applications of environmental and socio-economic data. Results showed that LUCCs have been significant in the Kashgar Region during the last 42 years. Cultivated land and urban/built-up lands were the most changed land cover (LC), by 3.6% and 0.4% from 1972 to 10.2% and 3% in 2014, respectively. By contrast, water and forest areas declined. Grassland and snow-covered areas have fluctuated along with climate and human activities. Bare land was changed slightly from 1972 to 2014. According to the land use transfer matrix, cultivated land replaced grass- and forestland. Urban/built-up land mainly expanded over cultivated and bare land. LUCCs were triggered by the interplay of natural and social drivers. Increasing runoff, caused by regional climate changes in seasonal variation, and snow melt water, have provided water resources for LC changes. In the same way, population growth, changes in land tenure, and socio-economic development also induced LUCCs. However, expansion of cultivated land and urban/built-up land led to increased water consumption and stressed fragile water systems during on-going climate changes. Therefore, the selection of adaption strategies relating to climate change and oasis development is very important for sustainable development in the Kashgar Region.

Keywords: arid region; LUCC; driving forces; snow index; SPOT VGT; Kashgar Region

1. Introduction

LUCC studies have emerged in research on global environmental changes via their interactions with climate, ecosystem processes, biogeochemical cycles, biodiversity, and human activities [1]. Therefore, for the last several years, numerous researchers have improved measurement of LUCCs by integrating environmental, human, and remote sensing/GIS science to answer various questions about LUCC and its driving forces [2]. Scholars believe the most common driving forces of LUCC have included population growth [3], human settlement and land tenure policy [4,5], changes in technology [6], culture [7], and political and economic changes [8]. Apart from that, climate-related

changes, such as rainfall variability [9], drought [10], and fire [11] were recognized as major LUCC drivers. While those research efforts have suggested that LUCC drivers differ depending on location, drivers remain contentious issues, and clearly their dynamics still requires analysis [12].

Located in the southwestern Xinjiang Uyghur Autonomous Region, China, the Kashgar Region is characterized by high mountains with snow/ice and an arid basin. Mountain uplift, westerly circulation, and the East Asian monsoon have determined its climate, creating a unique geographical unit—a mountain-alluvial plain-oasis-desert system. During the last half-century, rapid population growth and economic development have led to the modification of natural ecological processes. Increasing number of reservoirs and over-irrigation for cultivated land leads decreasing water flow in rivers by $1.5 \times 10^9 \text{ m}^3 \text{ year}^{-1}$. Consequently, a 240 km distance in the Kashgar and Yarkant Rivers has dried up, leading to the desert area's expansion towards the north [13]. Over-cutting of desert vegetation and trees along rivers resulted in the activation of 80% sand, which is moving towards the oasis at a rate of 5–10 m/year [14], and the salinization area has expanded into 59.17% of arable land ($3.38 \times 10^5 \text{ ha}$; [15]).

Water resources in the Kashgar Region depend mainly on snow melt from the mountain glacier, snow, and ice, which are major supply sources of surface runoff, ground water storage, and drinking water for the large population in this area. In the Kashgar Region, therefore, water is a major limiting resource, not only as a precious natural resource, but also as an important social factor for economic development [16]. Besides human activities, climate changes have also affected the hydrological cycle in the Kashgar Region. Global warming accelerates the process of atmospheric circulation and the hydrological cycle, subsequently affecting spatial and temporal distribution of water resources and exacerbating water shortages, especially in arid regions [17]. The occurrence of surface water in the Kashgar Region is strongly related to climatic, hydrological, and geomorphological factors.

In recent decades, increases in the Kashgar Region's social and economic activities and environmental changes have posed a great challenge to its sustainable development strategy, and extensive research has been conducted regarding this region. Anwaer et al. (2010) [18] analyzed total water uses in the Kashgar Region from 2001 to 2007. Results showed that agricultural water consumption increased most rapidly, from $76.78 \times 10^8 \text{ m}^3$ to $91.06 \times 10^8 \text{ m}^3$ during the six-year period. Anwaer et al. (2011) [19] also noted a significantly high correlation between urbanization and water utilization. Mansuer et al. (2011) [20] analyzed spatio-temporal dynamic changes of groundwater in the Kashgar Region, finding that cultivated land had been increasing continually, resulting in decreased groundwater levels midstream and downstream of the Kashgar and Yarkant Rivers, respectively. Rapid urbanization, socio-economic development, expansion of agricultural areas, and other anthropogenic activities played an important role in LUCCs. The Kashgar Region's arid environmental landscape has undergone tremendous LUCCs. However, the region's changes and drivers are not understood clearly. Most studies on the Kashgar Region have focused on individual factors, such as water stress [18,19], groundwater [20], and climate change [21]. However, few studies have shown that changes in climate and human activities have interacted over time to influence LUCC patterns in the region on different spatial and temporal scales. Therefore, this study's main objectives are to quantify LUCCs and to identify these changes' main driving forces. To achieve these goals, first LC maps are produced to provide a broad, synoptic perspective of land use measurements and mapping of environmental change. Then, investigation results of snow cover changes can strengthen knowledge of this region's water resources. Accumulation of snow cover and snow melt water are the main sources for rivers, groundwater recharges, and agriculture in the Kashgar Region. Finally, driving forces are identified based on integrated LC maps, snow cover monitoring, and environmental (temperature, precipitation, evaporation, and runoff) and socio-economic datasets (population, GDP, primary industry, and policy changes). This study's findings form a basis for a better understanding of the Kashgar Region's LUCCs and provide information to assist policymakers' decisions on future strategic management and sustainable development.

2. Materials and Methods

2.1. Study Area

The Kashgar Region, located in Northwest China, is in the southwest Xinjiang Uyghur Autonomous Region (Figure 1). The study area's administrative boundary lies within the range of $71^{\circ}39' - 79^{\circ}52'$ E and $35^{\circ}28' - 40^{\circ}18'$ N. Its administrative divisions include 11 counties and one city within a $113,913 \text{ km}^2$ area. According to 2014 census statistics, the total population was 4,683,114; the non-agricultural population accounts for 22.23%, and the agricultural population accounts for 77.66% [22]. Three mountains surround the Kashgar Region: Tainshan Mountain to the north, the Kunlun Mountain to the south, and the Pamir peaks to the west, stretching to $4.25 \times 10^4 \text{ km}^2$. Water vapor from the Indian Ocean and the Arctic Cold Front has difficulty penetrating the area due to the high mountain barriers. Thus, the study area has a typical inner-continental climate, with annual precipitation of less than 100 mm and evaporation of higher than 2000 mm annually in the plain, while permanent snow and glaciers exist at higher altitudes. The study area consists mainly of the Kashgar River and Yarkant River Alluvial Plains. The water supply along the Kashgar and Yarkant Rivers depends mainly on glaciers and snow melt water from the mountains. The average annual surface runoff of the Kashgar and Yarkant Rivers is 4.5 and $7.5 \times 10^9 \text{ m}^3$, respectively [23]. Water from these rivers is used mainly for irrigation, groundwater recharge, and hydropower generation.

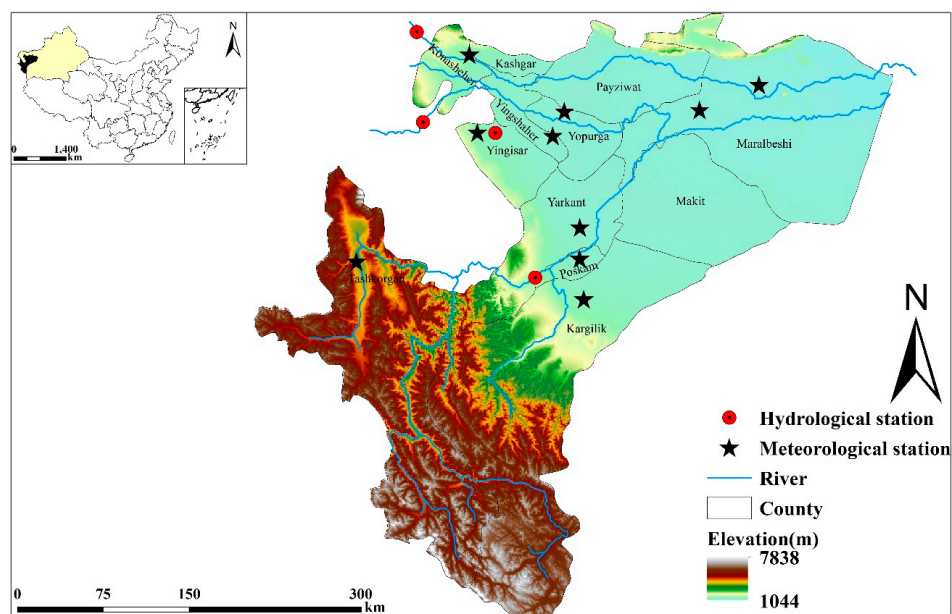


Figure 1. Location map of study area.

2.2. Data

In this study, we integrated the following different multi-spectral satellite images for LUCC analysis: Landsat Multispectral Scanner (MSS), Thematic Mapper (TM), Enhanced Thematic Mapper Plus (ETM+), Operation Land Imagery (OLI), and VGTATION images on board the SPOT-4. We further used natural and social statistical datasets to identify LUCCs' driving forces. Table 1 summarizes the characteristics of these datasets.

Table 1. Datasets used in this study.

Data Category	Sensor	Date	Resolution	Path/Row	Sources of Data
Remote sensing data	MSS	1972 (From June to October)	60 m	P147R32~P149/35	USGS
	TM	1990 (From June to September)	30 m	P147R32~P149/35	
	ETM+	2000 (From June to September)	30 m	P147R32~P149/35	
	OLI	2014 (From June to September)	30 m	P147R32~P149/35	
	SPOT-4	1 January 1999–30 May 2014	1 km	71°39'~79°52' E 35°28'~40°18' N	VITO
Hydrological data (annual runoff)	-	1964–2014	Station data	-	Karbal, Kirik, Kaqung Stations
Meteorological data (annual temperature, precipitation, evaporation)	-	1964–2014	Station data	-	Kashgar, Yarkant, Maralbeshi Tashkorgan stations
Statistical data	-	1984–2014	-	-	Xinjiang Statistical Year Book
Reference data	Google Earth	11 August 1972 Landsat 29 June 1973 Landsat 31 August 1990 Landsat 31 December 2000 Landsat 31 July 2013 Airbus 6 August 2013 Airbus 25 May 2014 Airbus 10 June 2014 Digital Globe 19 September 2014 Digital Globe		P147R32~P149/35	
		GDEM	17 October 2011	30 m	P147R32~P149/35

2.3. Methodology

2.3.1. Land Cover Mapping

Based on the study area's morphology and landscape, the possible appearance of LC types was considered to be 21 classes, and a hierarchical classification system of 21 classes was grouped into seven aggregated classes of LC: urban/built-up area, water area, grassland, cultivated land, forestland, snow/ice (considered only in summertime), and bare land. Table 2 provides detailed descriptions of each class. These classes' information was extracted using the maximum likelihood classification method combined with image segmentation (Figure 2). During summer seasons with cloud-free conditions, 48 Landsat images were acquired to map snow/ice and major LC types in the study area. Geometric correction was conducted by collecting for each image 40 well-conditioned ground control points, determined from topographic maps using ArcGIS. Root mean square (RMS) errors were less than 0.5 pixels for MSS (60 m), TM, ETM+, and OLI (30 m) images. MSS images were resampled to a 30 m cell size using the nearest-neighbor method. All images were geometrically corrected, with a reference system of a UTM map projection Zone 44 North on a WGS 1984 datum. In the initial step, we segmented band-stacked images into groups of pixels as objects. Homogenous pixel groups were created, which are called image objects, based on size, shape, and area. The multi-segmentation method utilized object-based classification because it generates objects very closely resembling ground features [24]. We implemented image segmentation using eCognition 9.0 to create objects that delineated LC classes. We applied two levels for the segmentation and classification process based on LC classes. Level 1 was applied for small and spread LC classes, such as grassland. The scale parameter was set at 5 [25]. Level 2 was applied for large LC classes, such as cultivated land, water, and bare land. The scale parameter was set at 10. Color and shape parameters were adjusted to 0.9 and 0.1, respectively [26]. After segmentation was completed, LC information was extracted with the maximum likelihood classification method [27]. Training sites were collected from original Landsat

data based on segmentation results, their different spectral features, Google Earth high-resolution images, and topographic maps, respectively. Because of the study area’s high mountains’ cloudy conditions during wintertime, collecting cloud-free Landsat images was difficult. Therefore, SPOT VGT imagery, chosen for mapping snow /ice cover due to its high temporal resolution and its maximum value composite (MVC) approach, helped minimized the effect of cloud cover [28]. The next section provides a detailed description of the snow/ice cover mapping process.

Table 2. Classification of land types in this study.

Classes	Definition
Urban/build-up area	Urban area, villages, industrial and commercial areas, transportation, communication and utilities
Cultivated land	Crop fields, cotton fields, vegetable lands, irrigated land, non-irrigated vegetation
Water	All areas of open water, rivers, streams, channels, lakes, reservoir and ponds, bottomland, swampland
Grassland	Dense grass, moderate grass, sparse grass,
Forest	Dense forest, scrubland, Sparse forest, orchards, groves, shrubland
Snow /ice	Glacier, snow, ice
Bare land	Desert, Gobi, salinized land, area of thin soil, rock, almost no vegetation cover

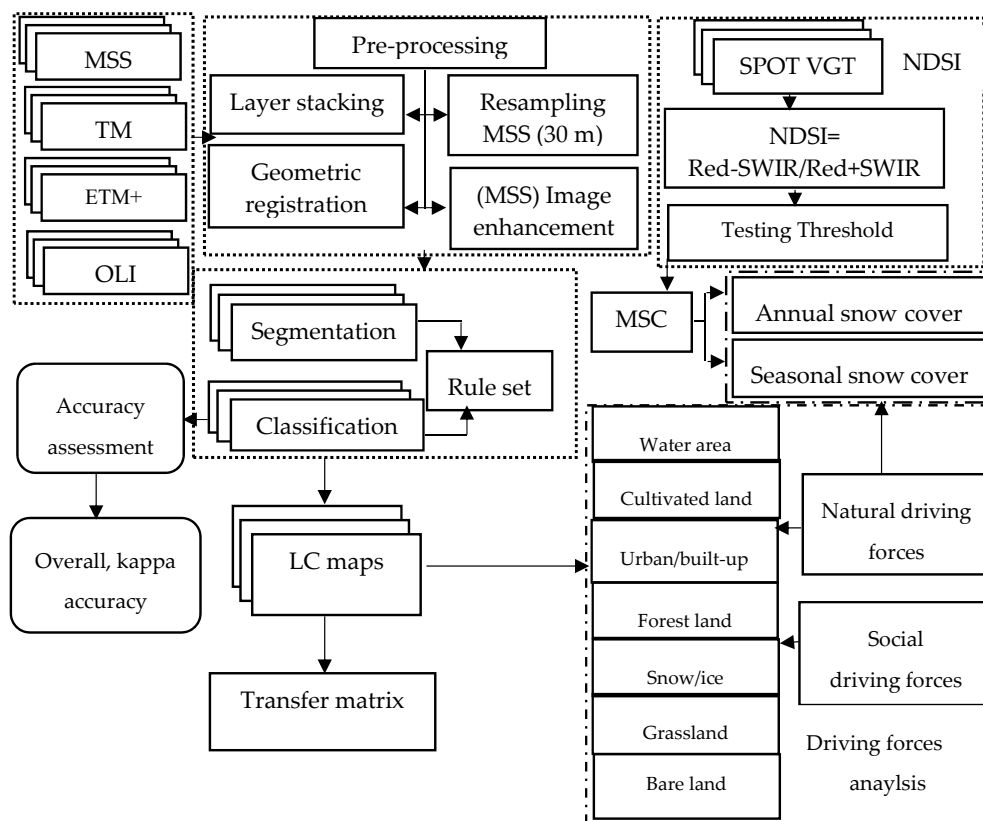


Figure 2. Flow chart of methodology.

2.3.2. Snow Cover Changes

Investigation of snow cover changes was completed in two steps, including the selection of critical threshold values for Normalized Difference Snow Index (NDSI) and threshold values from the NDSI index for extracting snow and ice information. VGT data have four spectral bands: B0 (blue, 430–470 nm), B2 (red, 610–680 nm), B3 (near infrared, 780–890 nm), and SWIR (short-wave infrared, 1580–1750 nm). Three standard VGT available products are VGT-P, VGT-S1, and VGT-S10. We applied the VGT-S10 (10-day synthesis product) data for snow cover mapping in this study. There are three 10-day composites for 1 month: days 1–10, 11–20, and day 21 to the last day of the month by

MVC [29]. The NDSI takes advantage of difference in reflectance of snow-covered and snow-free areas in near infrared and short-wave infrared bands [30,31]. The NDSI was calculated as follows:

$$\text{NDSI} = (\text{Red} - \text{SWIR}) / (\text{Red} + \text{SWIR}), \quad (1)$$

where Red and SWIR are band 2 and band 4 of digital numbers of SPOT VGT, respectively [32]. To determine whether a pixel is covered by snow or not, an observed pixel must meet a certain NDSI threshold value. A threshold value of 0.4 has been used to distinguish snow from bright soils, rocks, and clouds [32]. Kondoh and Suzuki [33] in 2005 modified the 0.4 of NDSI threshold using an NDVI adjustment to take into account forest effects on snow detection in Northern Eurasia. In this study, the original threshold value of 0.4 underestimated snow-covered areas. Therefore, several threshold values of 0.4, 0.3, and 0.2 were tested for NDSI, and the best agreement was found with a slightly lower threshold value of 0.2 (Figure 3). The best agreement for snow and ice pixels extraction using VGT data should correspond to broad snow-cover characteristics of the local area. Thus, a lower threshold value of 0.2 was adopted for VGT snow and ice detection in this study area. Then, 567 stages for the entire duration of time-series VGT data were collected to investigate snow cover changes from 1 January 1999 to 30 May 2014. From first year of September to the next year of August, 36 images were composited, representing the annual maximum snow cover area. Then, we averaged the annual areas to determine the annual average extent of snow cover in square kilometers. Seasonal snow cover variation was calculated quarterly: spring (March, April, May), summer (June, July, August), fall (September, October, November), and winter (December, January, November).

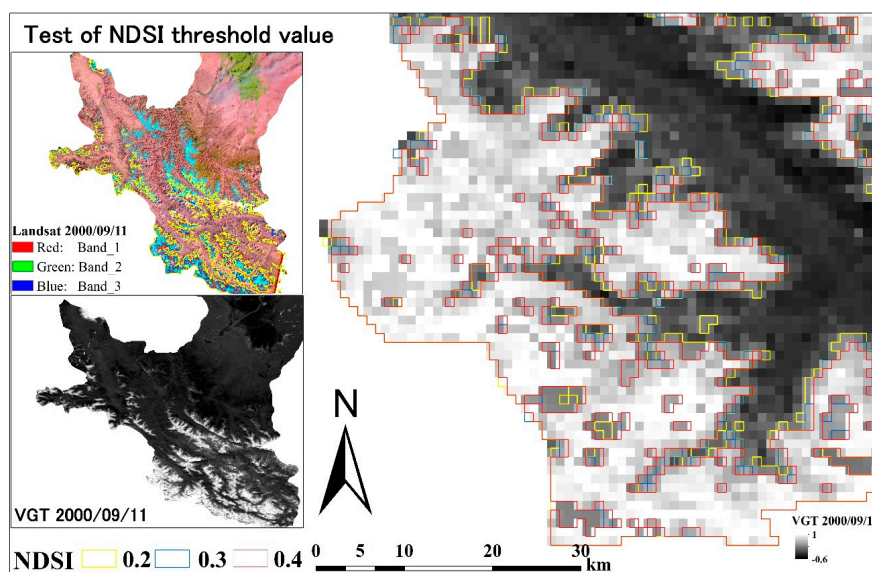


Figure 3. Test results of different threshold value for the Normalized Difference Snow Index (NDSI).

2.3.3. Accuracy Assessment

In this study, the accuracy assessment of image classification used the stratified random sampling design. Reference points were created randomly from classified maps of the study area for 1972, 1990, 2000, and 2014. A total of 700 points were selected randomly (100 points for each class). The original Landsat and Google Earth images were used as reference sources to classify the selected points. The reference points were confirmed by visual interpretation of the reference source, which were the only available reference data for evaluating the accuracy assessment. Overall accuracy, user accuracy, and the Kappa coefficient were computed from error matrices.

2.3.4. Trend Analysis with the Mann-Kendall Test for Hydro-Climate Variables

Characteristics of hydro-climatic changes in the Kashgar Region were analyzed based on data collected at four meteorological stations and three hydrological stations for the period of 1964–2014. The Mann-Kendall (MK) test can assess trends in a time series without requiring normality or linearity [34,35]; it is highly recommended for use by the World Meteorological Organization [36]. Therefore, the MK trend test has been widely used to test for randomness against trends in hydrology and climatology [37]. This study also used the MK trend test method, adapted by Xu et al. (2013) [38] to analyze trends in precipitation, temperature, evaporation, and annual runoff.

3. Results

3.1. Land Cover Mapping

Results of overall accuracy ranged from 88% to 91% (Table 3), and standard overall accuracy for LC maps has been established at 85% [39]. Kappa coefficient values ranged from 0.86 to 0.90; users and producers' accuracy for individual classes ranged from 100% to 65%. The grassland and forest's lowest accuracy could be explained by the area's aridity and sparse vegetation, which led to confusion between these LC types. However, the visual comparison method between the original satellite images and LC maps showed robust classification accuracy.

Table 3. Accuracy assessment of land cover (LC) map for 1972, 1990, 2000, and 2014.

Land Cover Classes	1972		1990		2000		2014	
	Users' Accuracy	Producers' Accuracy						
Urban	86%	67%	100%	95%	100%	91%	100%	68%
Water	100%	78%	97%	97%	100%	88%	100%	90%
Grassland	91%	91%	88%	65%	100%	69%	100%	96%
Cultivated land	80%	97%	89%	97%	94%	100%	91%	100%
Forestland	90%	60%	76%	73%	98%	91%	87%	81%
Snow/ice	100%	100%	100%	100%	100%	94%	100%	97%
Bare land	87%	100%	92%	100%	68%	100%	73%	100%
Overall accuracy	88%		93%		93%		91%	
Kappa statistic	0.86		0.92		0.91		0.90	

Each LC type's area changed significantly during the 42-year study period, as shown in Figure 4 and Table 4. Results indicate that cultivated land increased remarkably from 1972 to 2014, with its area reaching 11,677.5 km². This cultivated area results were compared with the sown area of XJSYB of Kashgar Region—as Figure 5 showed, the correlation was 0.9. Increased cultivated land led to increased water consumption and utilization of water resources. Water area has consistently decreased from 2762.9 km² (2.4%) in 1972 to 1062.4 km² (0.9%) in 2014. The urban/built-up area increased from 40.2 km² (0.4%) in 1972 to 392.8 km² (3%) in 2014. Increased population is associated with urban and built-up land expansion. The urbanization level (as the proportion of total population residing in the state's urban areas) increased from 19.63% in 2000 to 22.76% in 2014 [22].

Mainly distributed from the southern mountain to the northern plain in the study area, grasslands decreased from 4779.1 km² (4.1%) in 1972 to 2680.6 km² (2.3%) in 2000. In general, rainfall variability is a key driver of grassland changes in arid regions. Therefore, monthly precipitation data was observed in 2000 and 2014, respectively (Figure 6). In contrast, conversion of grassland to cultivated land and over-grazing are other reasons for grasslands' decreasing on the plain (Table 5; [40]). However, by 2014, grassland had increased to 3302.5 km² (2.9%). This trend was related to increasing precipitation in 2014 and the grassland restoration program launched in 2003. Figure 6 showed high precipitation in 2014, compared with 2000. In addition, the grassland restoration program mainly focused on improving the richness of local plant species in grasslands and controlling the stock density. Therefore, grasslands increased after in 2000.

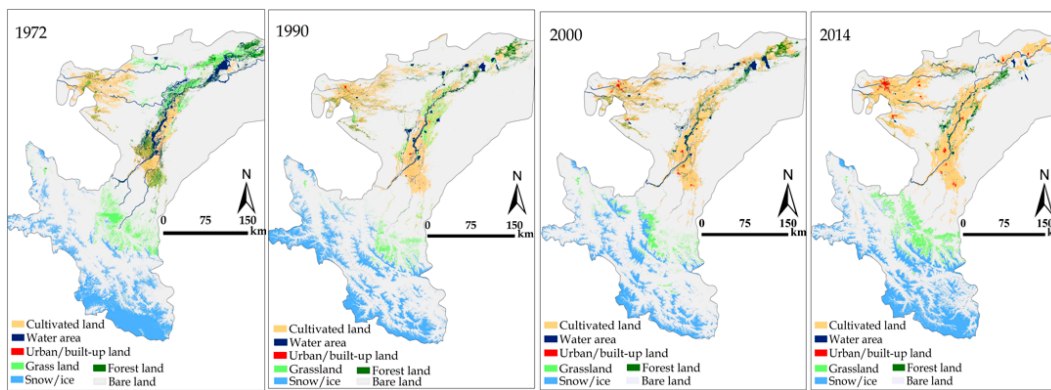


Figure 4. LC map of study area in 1972, 1990, 2000 and 2014.

Table 4. Results of land use/cover change (LUCC) statistics for 1972, 1990, 2000, and 2014.

Year	1972	1990	2000	2014				
Land Cover Class	Total Area (km²) Percentage (%)							
Water area	2762.9	2.4	1925.6	1.6	1291.2	1.1	1062.4	0.9
Cultivated land	4148.6	3.6	5991.4	5.2	6572.5	5.7	11,677.5	10.2
Urban/Built up	40.2	0.4	96.3	0.8	169.2	1.5	392.8	3
Grassland	4779.1	4.1	3701.3	3.2	2680.6	2.3	3302.5	2.9
Forest land	3584.5	3.1	2991.1	2.6	1545.7	1.3	1344.5	1.2
Snow/ice	10,838.8	10	10,789.5	9.4	8987.8	7.8	10,001.2	8.7
Bare land	87,558.4	77	88,417.0	77	92,665.5	80	86,131.7	74
Total area	113,912.5	100	113,912.5	100	113,912.5	100	113,912.5	100

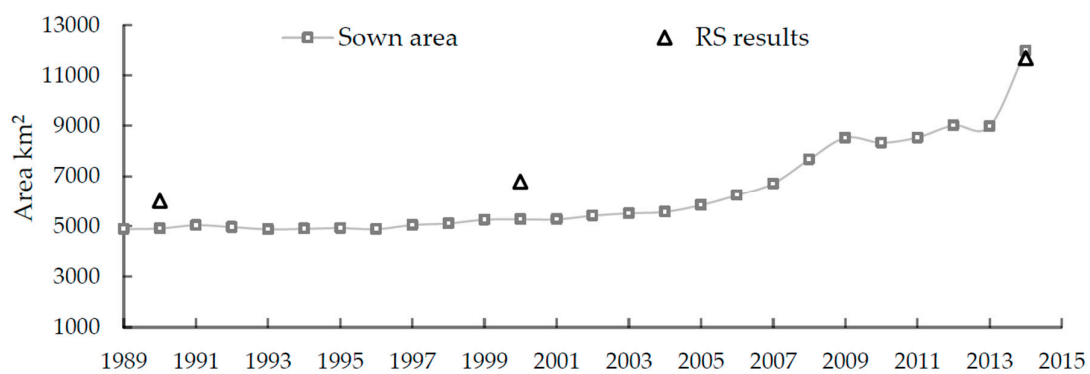


Figure 5. Sown area and remotely sensed (RS) estimated cultivated area comparison for Kashgar Region (sown area source [22]).

Conversely, from 1972 to 2014, forestland decreased from 3584.5 km² (3.1%) to 1344.5 km² (1.2%). Agricultural expansion was a key factor for forestland’s reduction. Forest area has mainly been distributed around the study area’s riverbanks, and it depends on groundwater resources, that is, groundwater seeping from a river. Therefore, forestland was easily converted into cultivated land due to abundant water resources for agricultural activity.

From 1972 to 2000, the area of snow/ice cover decreased slightly from 10,838.8 km² (10%) to 8987.8 km² (7.8%), but then increased to 10,001.2 km² (8.7%) in 2014. Overall, however, snow/ice cover shows a decreasing trend. Based on the First and Second Glacier Inventory of China, the glacier area in the Kashgar Region has shrunk by 927 km² due to global warming [41].

Bare land was the Kashgar Region’s most dominant LC, accounting for 77%–74% of its total overall area. Due to decreased of snow/ice, bare land remained at 92,665.5 km², or 80% of its 1990–2000 measurement. Bare land is characterized by sand, desert, and rock, so it is difficult to reclaim, as summarized in Table 2.

Furthermore, several observations can be made from time-series LC maps. Cultivated land: (i) expanded generally from west to east (the Kashgar River side); (ii) expanded along the banks of the Yarkant River; (iii) increased near the forest area; and (iv) expanded much more near the southern borders of the Yarkant River. These observations were mainly related to the study area’s topography and water resources because the flat alluvial plain could sustain increasing expansion of cultivated land and had sufficient water resources for agricultural production.

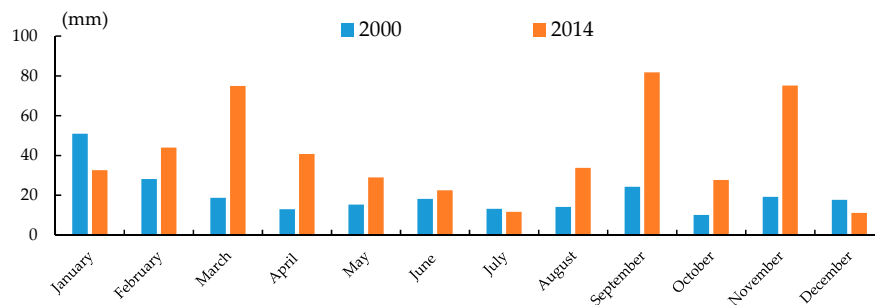


Figure 6. Monthly precipitation variation of mountain region in 2000 and 2014.

Table 5. Area transition matrix of Kashgar Region during 1972 to 2014.

Land Cover Classes in 1972 (km ²)	Land Cover Classes in 2014 (km ²)							Total
	Water	Cultivated Land	Urban/Built-up	Grassland	Forestland	Snow/Ice	Bare Land	
Water	954	151	0.01	157	70	456	974.8	2762.8
Cultivated land	27.1	2631	205.75	711	402	0.21	171.5	4148.5
Urban/built-up	0.23	5.9	28.99	0.1	0.02	0	5	40.2
Grassland	0.12	1913	13.6	2196	29.06	316	311.9	4779.6
Forestland	0.1	2328	10.74	9.4	843	52.4	340.8	3584.4
Snow/ice	1.45	1.6	0.00	38.9	0.19	8456	2340.6	10,838.7
Bare land	79.4	4647	133.4	189.9	0.01	720.6	81,987	87,757.4
Total 2014	1062.4	11,677.5	392.4	3302.5	1344.5	10,001.2	86,131.6	113,911.88

3.2. Snow Cover Changes

This research’s second aim was to investigate snow cover changes in the Kashgar Region, and Figure 7 shows those changes from 1999 to 2014. In general, a maximum snow-covered area exists in winter and spring when most snowfall has occurred but melting has not begun. As the summer season advances, depletion of snow-covered area occurs and temperatures increase. In this study region, annual snow cover variation was complicated and fluctuated greatly. Two high snowfalls occurred in the mountains of Kashgar and Yarkant in 2005 and 2009, respectively (Figure 7), most likely caused by an accumulation of winter and spring snowfall in those years. In contrast, low snow cover was recorded in 2007, and total snow cover tended to decrease, especially in the Yarkant River Mountain area, where it decreased remarkably year by year. The Mountains of Kashgar and the Yarkant River have a mean elevation above 4000 m, and the elevation of some mountains areas reaches 5000–6000 m—the terrain’s complexity results in great variations in distribution of temperature and precipitation. The mountain area has only one meteorological station (Tashkorgan, 3097.7 m). Annual mean precipitation is 450 mm in the high-elevation area (>5000 m) and 100 mm in the lower region (<3000 m). The long-term trend of temperature and precipitation increased at a rate of 0.72°C/10 year and 8.11 mm/10 year, respectively. Indeed, increasing temperature accelerated the melting and hindered the formation of glaciers, snow, and ice.

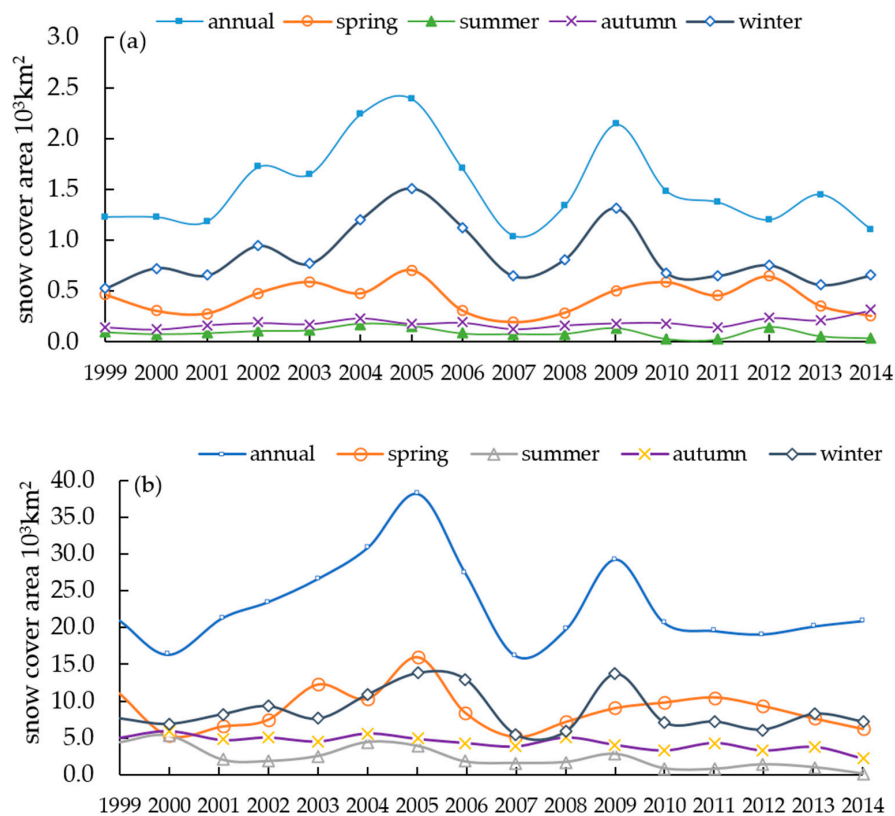


Figure 7. Annual and seasonal snow cover variation of Kashgar River (a) and Yarkant River (b).

4. Discussion

On a regional scale, the LUCC of oases is key to environmental change and has a cumulative effect in this arid land. LUCC in the arid region is mainly driven by unique natural and social factors [42,43]. Therefore, research on LUCCs' driving forces in the arid region is conducted by social and natural sciences, and requires an interdisciplinary approach. In this respect, research on the driving forces in the Kashgar Region focuses mainly on natural and human factors.

4.1. Natural Driving Forces of LUCC

The Kashgar Region covers a vast area; the region's southwest part is high, and its northeast part is low. Elevations in the study area divided into high and low mountains, plain, and desert areas. Due to differing characteristics of temperature and precipitation in these areas, we selected four observation stations for investigating characteristics of climate variables: Kashgar (1288.7 m, in the north), Maralbishi (1116.5 m, in the east), Yarkant (1231 m, in the south), and Tashkorgan (3093.7 m, in the mountains). As with the results of MK trend tests, all variables showed significant increasing trends, except for evaporation on the mountains (Table 6). These results indicated that during the past 50 years, the climate exhibited a warming trend. Other scholars have observed a similar trend in the northwest Xinjiang Region over the last 30 years [44].

In general, temperatures on the plain (Kashgar, Maralbeshi, and Yarkant) are higher than in the mountain ranges (Tashkorgan). On the one hand, increasing temperatures have favored agricultural production, and cotton production average yield per acre increase 373.5 kg hm^{-2} per decade from 1990 to 2013 [45]. Cultivated land increased from 4148.6 km^2 in 1972 to $11,677.5 \text{ km}^2$ in 2014 (Table 4). On the other hand, increasing temperatures enhanced transpiration and evaporation of crop and surface water. Evaporation on the plain ranged from 0.02 to 0.04 (Table 6), indicating a significant increasing trend. Expansion of cultivated land led to increased water consumption, from $50 \times 10^8 \text{ m}^3$ to $155 \times 10^8 \text{ m}^3$ from 1950 to 2010 [22], and increasing utilization of surface water. LUCC results

indicated that surface water decreased from 2762.9 km² to 1062.4 km² (Table 4), possibly caused by increased temperature and agricultural water consumption.

Table 6. The results of the Mann-Kendall test for climatic-hydro variables.

	Kashgar *		Maralbishi *		Yarkant *		Tashkorgan *		Kaqun +		Karbel +		Kirik +	
	Zc	β	Zc	β	Zc	β	Zc	β	Zc	β	Zc	β	Zc	β
T	5.01	0.11	3.14	0.02	4.13	0.03	2.09	0.04	-	-	-	-	-	-
P	2.59	0.57	3.05	0.12	3.19	0.46	4.15	0.23	-	-	-	-	-	-
E	3.10	0.02	3.15	0.04	2.04	0.04	-0.54	-0.04	-	-	-	-	-	-
R	-	-	-	-	-	-	-	-	0.64	0.11	1.2	0.1	1.19	0.36

Note: * meteorological station; + hydrological station; T-temperature, P-precipitation, E-evaporation, and R-runoff; Zc-standard normal random variable. β-Kendall slope, a positive β is rising trend, while a negative β means a decreasing trend.

In the mountainous areas, high-elevation glaciers and snow cover provide annual runoff and groundwater in the Kashgar Region. Seasonal runoff patterns were heavily dominated by winter snow accumulation and spring melt. Generally, snow cover is a seasonal phenomenon, and its variability is higher than that of glaciers. The air temperature is a major index for the snow and ice melt process, due to snow's particular sensitivity to climate changes. An increase of 2 °C in air temperature had a much more important effect on snow cover than doubling the precipitation during the snowmelt period [46]. Figure 8a displays the increased mountain temperatures over time. As temperatures rise, more precipitation falls as rain instead of snow, leading to smaller snowpack, decreased proportion of solid precipitation, and enhanced snowmelt. Figure 7 displays the slightly decreasing trend in annual snow cover. Then, rising temperatures have caused changes in snow cover that contributed to increased natural runoff of the Kashgar and Yarkant Rivers. The MK test results in Table 6 and Figure 9 indicate that runoff has increased. Particularly during the observation period from 1999 to 2014, snow cover changes have had strong effects on runoff discharge, and runoff displays an increasing trend, with pronounced peaks having occurred in 2005 and 2009. The relationship among snow cover, runoff, precipitation, and temperature on short- and long-term scales have been analyzed based on the only available annual data (snow cover, precipitation, temperature, and runoff). The high snow cover accumulations recorded in 2005 and 2009 (Figure 7) was attributed to annual precipitation in the mountain range in the same years (Figure 8b). During the same time, temperatures of the study area recorded their higher peak in mountain (Figure 8a). Increased temperatures might have accelerated snowmelt and contributed to the increased runoff in 2005 and 2009 (Figure 9) on the short-term scale. Yan et al. (2007) [47] showed that regional runoff increased by 10–16% when temperature rose by 1 °C, based on the correlation between temperature and the Yarkant River's monthly mean discharge. The magnitude of glacier contribution to natural runoff is much less than snow melt runoff in the short-term. However, Dong et al. (2009) [48] addressed the long-term effect of temperature and precipitation changes on physical characteristics of the area's glaciers. With an increase in air temperature during the study period (1960–2000), glaciers in the Yarkant River basin retreated by 6.1% and overcame effects of increased precipitation on the glacier mass balance due to regional climate changes that enhanced glacier ablation, which provided melt water for a longer time. In addition, Chen et al. (2006) [49], Xu et al. (2009) [50], and Qiang et al. (2010) [51] have addressed hydro-meteorological processes by investigating changing characteristics of precipitation, temperature, and runoff. Their results indicated significant runoff increases due to climate changes of the Yarkant and Kashgar Rivers. As discussed above, snow and glacier contributions form a major part of total runoff in the Kashgar Region, and therefore changes in snow and glacier melt runoff due to climate change are reflected in changes of the total stream flow of those rivers. Natural runoff from melting snow and ice has played an important role in the recharge of groundwater infiltration and storage. The total natural recharge of groundwater is 89.3×10^8 m³/year in the Kashgar Region [52].

Replenishment by precipitation is not very significant to groundwater in this study area’s arid climate. The geographical distribution of runoff has changed due to increased human activities, which may have affected replenishment of groundwater and changes to the changes of total stream flow of those rivers.

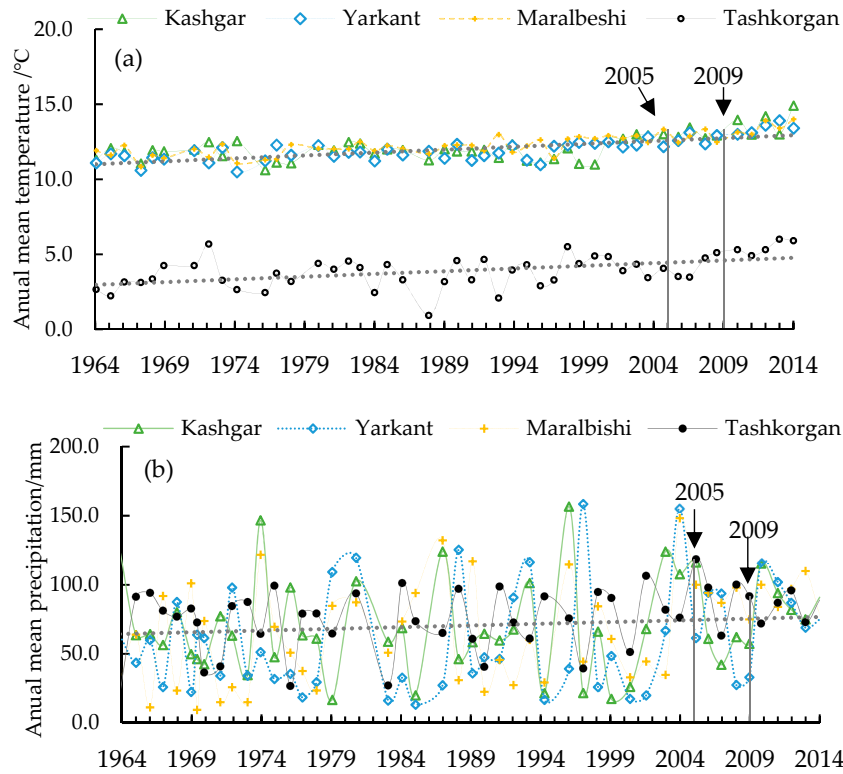


Figure 8. Annual mean temperature (a); and precipitation (b) trend of Kashgar Region.

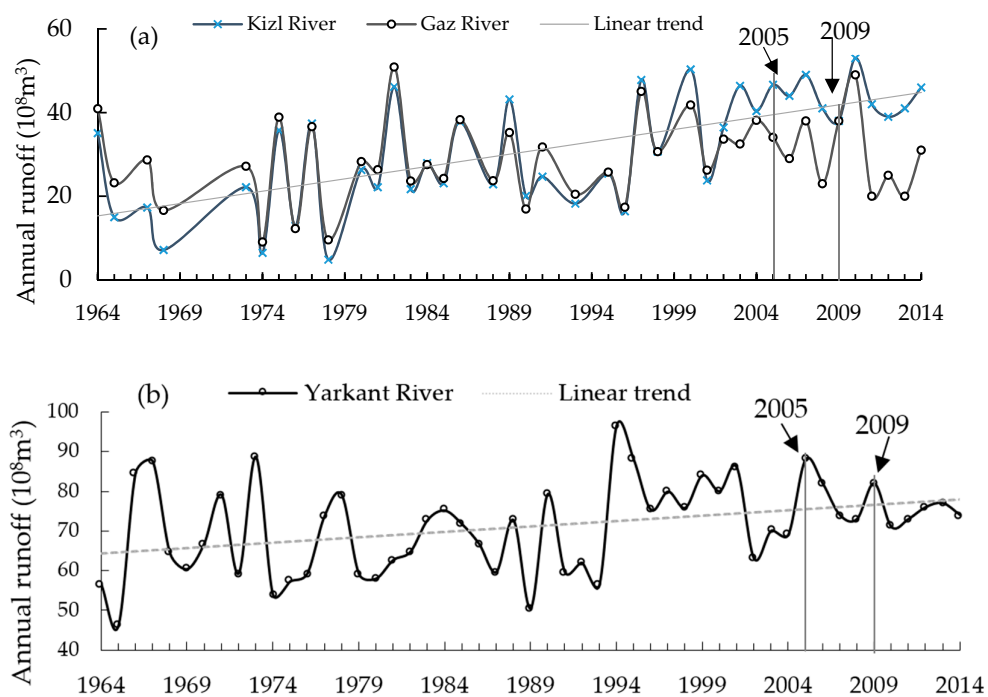


Figure 9. Runoff variation of Kashgar River (a); and Yarkant River (b).

4.2. Social Driving Forces of LUCC

4.2.1. Impact of increasing of population on LUCCs

Population growth has been identified as a major driving force for agricultural expansion and water consumption by Zhou et al. (2003) [53], Zhang et al. (2003) [54], Wang et al. (2008) [55], and Til et al. (2015) [56] for different areas in arid Northwest China. The population of the Kashgar Region rose from 2,745,362 in 1988 to 4,683,114 in 2014 [22], an increase of approximately 70%. Generally, the growing population has requested more land for basic needs of living, such as food and housing. More than 78% of households in rural areas depend largely on land resources, and agriculture contributes a large share of the gross domestic product (GDP). Crop and cotton production has increased, and the total agricultural area has expanded. Figure 10 shows the population increase in the Kashgar Region. A high positive correlation was found between population and sown area. The majority of grassland and forestland was occupied by cultivated land to satisfy people's demand for food (Table 6). As a result, grassland decreased from 4779.1 km² in 1972 to 2680.6 km² in 2000, and forest decreased from 3584.5 km² in 1972 to 1344.5 km² in 2014. Bare land and cultivated land were converted to urban/built-up land, which increased from 40.2 km² in 1972 to 392.8 km² in 2014. Population growth resulted in the expansion of cultivated land, with reclamation and evident shrinkage of grass and forest cover. Therefore, population is a major factor in LUCCs.

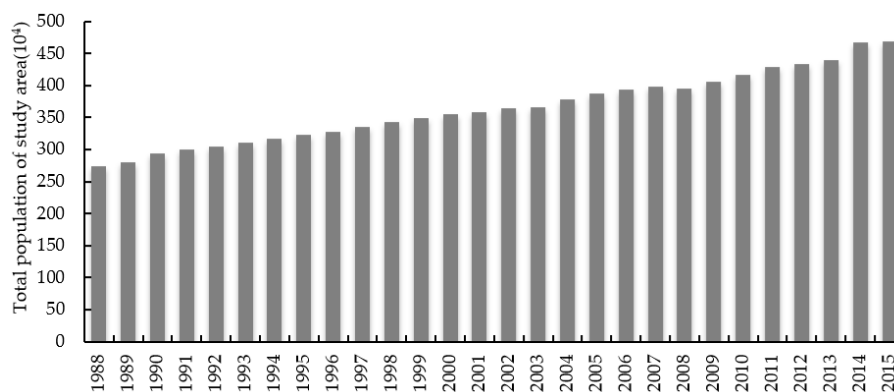


Figure 10. Total population of study area (source: [22]).

4.2.2. Impact of Policy-Induced Agricultural Land Development on LUCCs

Policy has contributed directly to the area's economy because political and economic activities are strongly interlinked with economic needs. Moreover, economic pressures were reflected in political programs, and economic instruments were used to implement political driving forces. Socio-economic developments of the Kashgar Region have been observed from 1984 to 2014, during which time the average annual growth rate of the GDP and primary industry increased by 138% and 35%, respectively (Figure 11). Policy influences on LUCCs in the Kashgar Region have been demonstrated based on document analysis, that is, international scientific literature, national studies, and government reports. Policy influences were closely associated with LUCC driving factors observed in the study area. For clarity, we organized these major events into the following three distinct historical periods.

First period, 1979–1984: The land tenure system adopted an 'open-door policy'. This policy led to the distribution of land from proprietors to individual households according to land tenure [57]. Consequently, land tenure policy has impacted agricultural production's efficiency and the region's economic development. The primary change in LUCC was the expansion of cultivated land near the alluvial plain (LC map for 1972, Figure 4). Government plans supported this expansion of agriculture and provided opportunities for expansion of grain and crop cultivation, which has initially supported the population's food and economic desires.

Second period, 1984–1990s: This period includes the most significant changes to land policy. The bureau of land administration was established and became responsible for land allocation, acquisition, monitoring, development, and for implementations of land law. Administrative law has legalized individual access to owning land in an attempt to develop the land market in Xinjiang and the inner cities of China. Individual ownership was implemented to promote socio-economic development and further improve people’s living standards. Agriculture attracted the attention of land businesspeople. Because of rising market prices, cotton cultivation brought fast economic growth. China became a global leading textile and clothing exporter, with rising demand for cotton driving prices to historically high levels [58]. The Kashgar Region has accounted for 43% of Xinjiang cotton production, and responses to cotton market expansion resulted in cultivating more land there.

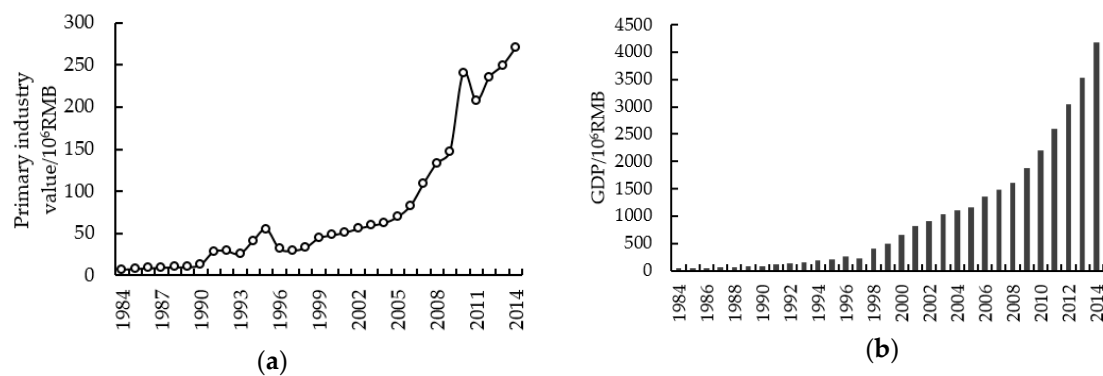


Figure 11. Primary industry (a); and gross domestic product (GDP) (b) of study area (source: [22]).

The general pattern of agricultural expansion from 1984 to 1990 in the plains and along the rivers has continued and led to intensified land use (LC map for 1990, Figure 4). The change in the distribution of land use, especially the expansion of cultivation around critical water resources, has resulted in the agricultural sector’s increased demand for water. Thus, the government has increased investment to establish irrigation channels, and the pattern of expansion along irrigation channels has led to continually increasing agricultural production. The Kashgar Region’s increasing agricultural output has also led to the construction of transport corridors—a long southern Xinjiang railway and a national highway from Kashgar to other domestic markets. These corridors, in turn, have led to increased economic linkages between the Kashgar Region and surrounding cities [59].

Current period, 2000s–2014: The government announced the abolition of the agricultural tax [60] and an adjustment of crop and cotton production structures towards market requirements. In addition, in 2001, China joined the World Trade Organization, which supports the agricultural sector [61]. Since 2002, China has implemented direct agricultural income and agricultural machinery subsidies. For these reasons, since 2005, the Kashgar Region’s primary industry has undergone dramatic changes (LC map for 2000 and 2014, Figure 4). Moreover, the government launched special economic development zones along the Kashgar River to attract domestic and foreign investment. The main goal of this economic zone is to boost economic development in the Kashgar Region by providing favorable policies such as tax exemptions, energy supplies, and access to transportation in 2011 [62]. Consequently, in 2013, China and several Central Asian countries cooperated to build the ‘Silk Road Economic Belt’ for mutual commercial benefits [63]. These on-going political and new economic events have altered LUCCs (such as opened the new land for cultivation, Figure 12) by local- and national-level approaches to the Kashgar Region’s development. These external drivers, combined with local situations, have contributed to LUCCs.

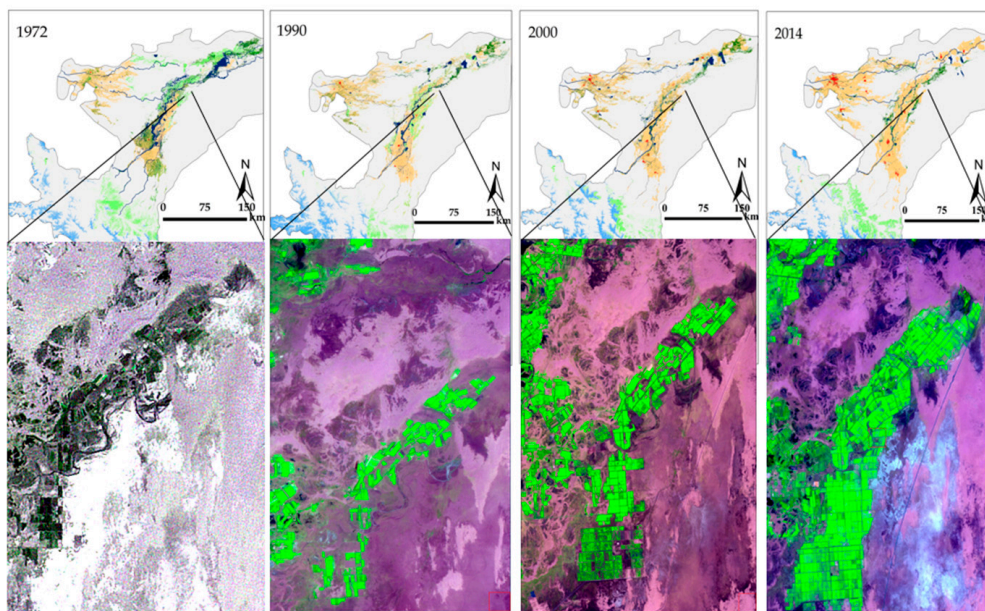


Figure 12. Opened new cultivated land continually from 1972 to 2014.

5. Conclusions

In Kashgar Region, agricultural and economic development in oasis mainly depends on melt-water from glaciers and seasonal snow in the high mountain areas. Knowledge of quantifying LUCC and its driving forces including natural and social drivers determined by anthropogenic and climate change are essential for sustainable development in this region. We combined multi-scale (Landsat) and multi-temporal (SPOT VGT) remotely sensed images to investigate spatial and temporal dynamics of LUCCs, including snow cover changes, during the last 42 years (1972–2014). The results showed that water, forest, grassland, and bare land have exhibited declining trends due to the expansion of cultivated and urban/built-up land from 3.6%, 0.4% to 10.2%, and 3%, respectively. Snow/ice covered areas have fluctuated, considering that only snow area in the summer time first decreased and then increased, according to the Landsat snapshot. However, the total snow covered slightly decreased, as confirmed by the SPOT VGT time-series data analysis.

The increasing of temperature and precipitation have different effects on plain and mountain areas. In the plain areas, increasing temperature has increased evaporation and water consumption, but inter-annual changes in precipitation had less impact on LUCCs. Meanwhile, in mountain areas, both of them especially experienced warming and decreased snow cover, which led to increased natural runoff, providing water resources in the plain.

Besides natural factors, demands from the growing population for basic needs of living and economic development were the anthropogenic drivers of LUCCs. Policy-related agricultural expansion shifted land use from small- to large-scale intensive farming. These drivers were the primary drivers of LUCCs in the Kashgar Region. At the same time, changes to the temperature, snow cover, and runoff was a facilitator of implementing anthropogenic driving forces. This study's results are valuable in the Kashgar Region and other arid regions with similar geographic conditions.

Acknowledgments: Ayisulitan Maimaitiaili would like to express and most sincere gratitude go to the Kawashima Shoji Memorial Scholarship Fund for financially supporting during the study period of this research.

Author Contributions: Main part of this study was performed by Ayisulitan Maimaitiaili and she wrote this paper; XiaoKaiti Aji and Akbar Matniyaz gave key suggestions, especially methodology and conclusions part during this study. Akihiko Kondoh was her supervisor during this study and provided invaluable guidance on technical aspects of this study, as well as improving this manuscript.

Conflicts of Interest: I declare that the authors of this paper no conflict of interest.

References

1. Townshend, J.R. *Improved Global Data for Land Applications*; IGBP Report 20; International Geosphere-Biosphere Programme: Stockholm, Sweden, 1992.
2. Lambin, E.F.; Baulies, X.; Bockstael, N.; Fischer, G.; Krug, T.; Leemans, R.; Moran, E.F.; Rindfuss, R.R.; Sato, Y.; Skole, D.; et al. *Land-Use and Land-Cover Change (LUCC): Implementation Strategy*; IGBP Report 48, IHDP Repot 10; International Geosphere-Biosphere Programme: Stockholm, Sweden; International Human Dimensions on Global Environmental Change Programme: Bonn, Germany, 1999; p. 125.
3. Lambin, E.F.; Turner, B.L.; Geist, H.J.; Agbola, S.B.; Angelsen, A.; Bruce, J.W.; Xu, J. The causes of land-use and land-cover change: Moving beyond the myths. *Glob. Environ. Chang. Hum. Policy Dimens.* **2001**, *11*, 261–269. [[CrossRef](#)]
4. Murphree, M.W.; Cumming, D.H.M. Savanna land use: Policy and practice in Zimbabwe. In *The World's Savanna's: Economic Driving Forces, Ecological Constraints and Policy Options for Sustainable Land Use*; UNESCO and Parthenon Publishing Group: Paris, France, 1993; pp. 139–178.
5. Blaikie, P.; Brookfield, H. *Land Degradation and Society*; Methuen: New York, NY, USA, 1987.
6. Grübler, M.A.; Meyer, W.B.; Turner, B.L. *Changes in Land Use and Land Cover: A Global Perspective*; University of Cambridge: Cambridge, UK, 1994; pp. 287–328.
7. Rockwell, R.C. Culture and cultural change. In *Changes in Land Use and Land Cover: A Global Perspective*; Cambridge University Press: Cambridge, UK, 1994; pp. 357–359.
8. Sanderson, S. Political-Economic Institutions. In *Changes in Land Use and Land Cover: A Global Perspective*; Meyer, W.B., Turner, B.L., Eds.; Cambridge University Press: Cambridge, UK, 1994; p. 369.
9. Yang, Y.; Feng, Z.; Huang, H.Q.; Lin, Y. Climate induced changes in crop water balance during 1960–2001 in Northwest China. *Agric. Ecosyst. Environ.* **2008**, *127*, 107–118. [[CrossRef](#)]
10. Román-Cuesta, R.M.; Carmona, M.C.; Lizcano, G.; New, M.; Silman, M.; Knoke, T.; Malhi, Y.; Oliveras, I.; Asbjornsen, H.; Vuille, M. Synchronous fire activity in the tropical high Andes: An indication of regional climate forcing. *Glob. Chang. Biol.* **2014**, *20*, 1929–1942. [[CrossRef](#)] [[PubMed](#)]
11. Kicklighter, D.W.; Cai, Y.; Zhuang, Q.; Parfenova, E.I.; Paltsev, S.; Sokolov, A.P.; Melillo, J.M.; Reilly, J.M.; Tchebakova, N.M.; Lu, X. Potential influence of climate-induced vegetation shifts on future land use and associated land carbon fluxes in northern Eurasia. *Environ. Res. Lett.* **2014**, *9*, 35004. [[CrossRef](#)]
12. Beilin, R.; Lindborg, R.; Stenseke, M.; Pereira, H.M.; Llausàs, A.; Slätmo, E.; Cerqueira, Y.; Navarro, L.; Rodrigues, P.; Reichelt, N.; et al. Analysing how drivers of agricultural land abandonment affect biodiversity and cultural landscapes using case studies from Scandinavia, Iberia and Oceania. *Land Use Policy* **2014**, *36*, 60–72. [[CrossRef](#)]
13. Zhen, D.Z. Concept, cause and control of desertification in China. *Quaternaryes* **1998**, *18*, 145–155. (In Chinese)
14. Nian, F.L.; Jie, T. *Comprehensive Study of Ecological Environmental Geology in the Western Plain of the Tarim Basin of China*; Jilin University Publishing House: Changchun, China, 1992; pp. 89–185. (In Chinese)
15. Guo, Q.Z. Study of the cycle of materials in soil-sphere and soil development. *Soil* **1991**, *123*, 1–3. (In Chinese)
16. Jia, B.Q. Approach to some theoretical problem on oasis landscape. *Arid Land Geogr.* **1996**, *16*, 56–65. (In Chinese)
17. Chen, Y.N.; Li, B.F.; Li, Z.; Li, W.H. Water resources formation and conversion and water security in arid region of Northwest China. *J. Geogr. Sci.* **2016**, *26*, 939–952. [[CrossRef](#)]
18. Anwaer, M.; Zhang, X.L.; Tashkin, J. Temporal and Spatial of Water Use and the Driving Mechanism in Kashgar District, Xinjiang. *J. Beijing Norm. Univ. (Nat. Sci.)* **2010**, *46*, 202–207. (In Chinese)
19. Anwaer, M.; Zhang, X.L.; Yang, D.G. Grey Relational Analysis of Change of Urbanization and Water Use Structure in Kashkar District, Xinjiang. *J. Desert Res.* **2011**, *31*, 261–266. (In Chinese)
20. Mansur, S.; Abulimiti, A.; Reyihangul, W. Cultivated land change and its ground water level response in kashghar in last decade. *J. Arid Land Resour. Environ.* **2011**, *25*, 145–151. (In Chinese)
21. Abudoukerimu, A.; Qin, R.; Yilidarjiang, T.; Xin, Z.F. Climatic variation characteristics in Kashi Region during 1961–2010. *Desert Oasis Meteorol.* **2012**, *6*, 34–40. (In Chinese)
22. National Bureau of Statistics. *Xinjiang Statistical Year Book (1984–2014)*; China Statistical Press: Beijing, China, 2016.

23. Li, P.Y. Evaluation and rational development and utilization of water resources in the Xinjiang Uigur Autonomus Region. *Arid Land Geogr.* **1987**, *110*, 13–48. (In Chinese)
24. Definiens. *Definiens Professional 5 User Guide*; Definiens AG: München, Germany, 2006; p. 15.
25. Abdullah, F.A.; Lalit, K.; Priyakant, S. Urban land cover change modelling using time-series satellite images: A case study of urban growth in five cities of Saudi Arabia. *Remote Sens.* **2016**, *8*, 838. [[CrossRef](#)]
26. Yu, W.; Zhou, W.; Qian, Y.; Yan, J. A new approach for land cover classification and change analysis: Integrating backdating and an objective-based method. *Remote Sens. Environ.* **2016**, *177*, 37–47. [[CrossRef](#)]
27. Benedicsson, J.A.; Swain, P.H.; Ersoy, O.K. Neural network approaches versus statistical methods in classification of multisource remote sensing data. *IEEE Trans. Geosci. Remote Sens.* **1990**, *28*, 540–551. [[CrossRef](#)]
28. Xiang, M.X.; Stephen, B.; Ji, Y.L.; Da, F.Z.; Ming, L.L. Characterization of forest types in Northeastern China, using multi-temporal SPOT-4 VEGETATION sensor data. *Remote Sens. Environ.* **2002**, *82*, 335–348. [[CrossRef](#)]
29. Vegetation User Guide. Available online: <http://www.spot-vegetation.com/userguide/userguide.htm> (accessed on 9 June 2011).
30. Crane, R.G.; Anderson, M.R. Satellite discrimination of snow/cloud surfaces. *Int. J. Remote Sens.* **1984**, *5*, 213–223. [[CrossRef](#)]
31. Xiao, X.; Moore, B.; Qin, X.; Shen, Z.; Boles, S. Observations of alpine snow and ice cover in Asia: Using multi-temporal VEGETATION sensor data. *Int. J. Remote Sens.* **2002**, *23*, 2213–2228. [[CrossRef](#)]
32. Hall, D.K.; Crawford, C.J.; DiGirolamo, N.E.; Riggs, G.A.; Foster, J.L. Development of methods for mapping global snow cover using Moderate Resolution Imaging Spectroradiometer Data. *Remote Sens. Environ.* **1995**, *54*, 127–140. [[CrossRef](#)]
33. Kondoh, A.; Suzuki, R. Snow cover mapping and its interannual variation in Northern Eurasia, Japan. *J. Jpn. Soc. Hydrol. Water Resour.* **2005**, *18*, 695–702. (In Japanese) [[CrossRef](#)]
34. Kendall, M.G. *Rank Correlation Methods*, 4th ed.; Charles Griffin: London, UK, 1975.
35. Mann, H.B. Non-parametric test against trend. *Econometrica* **1945**, *13*, 245–259. [[CrossRef](#)]
36. Mitchell, J.M.; Dzerdzevskii, B.; Flohn, H.; Hofmeyr, W.L.; Lamb, H.H.; Rao, K.N.; Wallen, C.C. *Climate Change*; WMO Technical Note No. 79; World Meteorological Organization: Geneva, Switzerland, 1966; p. 79.
37. Partal, T.; Kahya, E. Trend analysis in Turkish precipitation data. *Hydrol. Process.* **2006**, *20*, 2011–2026. [[CrossRef](#)]
38. Xu, J.H.; Chen, Y.N.; Li, W.H.; Nie, Q.; Hong, Y.L.; Yang, Y. The nonlinear hydro-climatic process in the Yarkant River, northwest China. *Stoch. Environ. Res. Risk Assess.* **2013**, *27*, 389–399. [[CrossRef](#)]
39. Anderson, J.R.; Hardy, E.E.; Roach, J.T.; Witmer, R.E. *A Land Use and Land Cover Classification System for Use with Remote Sensor Data*; Geological Survey U.S.: Listeria, VA, USA, 1976; Volume 964, p. 28.
40. Chen, L. Analysis on Interannual Variation of Different Grassland Types in Tashkurgan County. *Pratacult Anim. Husb.* **2010**, *9*, 18–21. (In Chinese)
41. Ke, Q.D.; Bai, Q.X.; Guan, J.W. Snow accumulation variability at altitude of 7010m a.s.l. in Muztag Ata Mountain in Pamir Plateau during 1958–2002. *J. Hydrol.* **2015**, *531*, 912–918. [[CrossRef](#)]
42. Luo, G.P.; Zhou, C.; Chi, X. Process of land use/land cover change in the Oasis of Arid Region. *Acta Geogr. Sin.* **2003**, *58*, 63–72. (In Chinese)
43. Hietel, E.K.; Waldhardt, R.N.; Otte, A.N. Linking socio-economic factors, environment and land cover in the German Highlands, 1945–1999. *J. Environ. Manag.* **2005**, *75*, 133–143. [[CrossRef](#)]
44. Chen, Y.N.; Li, Z.; Fan, Y.T.; Wang, H.J.; Deng, H.J. Progress and prospects of climate change impacts on hydrology in the arid region of northwest China. *Environ. Res.* **2015**, *139*, 11–19. [[CrossRef](#)] [[PubMed](#)]
45. Abudoukerimu, A.; Hu, S.Q.; Nuerpatiman, M.R. Analysis on the Impact of Climate Change on Yield and Yield of Cotton in Kashgar, Xinjiang. *Chin. J. Eco-Agric.* **2015**, *23*, 919–930. (In Chinese)
46. Rango, A.; Martinec, J. Areal extent of seasonal snow cover in a changed climate. *Nord. Hydrol.* **1994**, *25*, 233–246.
47. Jiang, Y.; Zhou, C.H.; Cheng, W.M. Streamflow trends and hydrological response to climatic change in Tarim headwater basin. *J. Geogr. Sci.* **2007**, *17*, 51–61. [[CrossRef](#)]
48. Dong, H.S.; Shi, Y.L.; Yong, J.D.; Lian, F.D.; Jun, L.X.; Li, J. Glacier changes during the last forty years in the Tarim Interior River Basin, northwest China. *Prog. Nat. Sci.* **2009**, *19*, 727–732. [[CrossRef](#)]
49. Chen, Y.N.; Takeuchi, K.; Xu, C.C.; Chen, Y.P.; Xu, Z.X. Regional climate change and its effects on river runoff in the Tarim Basin, China. *Hydrol. Process.* **2006**, *20*, 2007–2216. [[CrossRef](#)]

50. Xu, C.C.; Chen, Y.N.; Hamid, Y.M.; Tashpolat, T.Y.; Chen, Y.P.; Ge, H.T.; Li, W.H. Long-term change of seasonal snow cover and its effects on river runoff in the Tarim River basin, northwestern China. *Hydrol. Process.* **2009**, *23*, 2045–2055. [[CrossRef](#)]
51. Zhang, Q.; Xu, C.; Tao, H.; Jiang, T.; Chen, Y. Climate changes and their impacts on water resources in the arid regions: A case study of the Tarim River Basin, China. *Stoch. Environ. Res. Risk Assess.* **2010**, *24*, 349–358. [[CrossRef](#)]
52. Lin, N.-F.; Tang, J.; Han, F.-H. Eco-environmental problems and effective utilization of water resources in the Kashi Plain, western Terim Basin, China. *Hydrogeol. J.* **2001**, *9*, 202–207. [[CrossRef](#)]
53. Zhou, Y.; Wang, J.; Ma, A.; Qi, Y.; Bayea, Y. Study on land use dynamics based on RS and GIS in Linze County. *J. Desert Res.* **2003**, *23*, 142–146. (In Chinese)
54. Zhang, H.; Wu, J.; Zheng, Q.; Yu, Y. A preliminary study of oasis evaluation in the Tarim Basin, Xinjiang, China. *J. Arid Environ.* **2003**, *55*, 545–553. [[CrossRef](#)]
55. Wang, Y.; Xi, X.; Li, Y.; Xu, H. Analysis of the land-using and environmental effect in the middle reach of the Tarim River. *J. Anhui Agric. Sci.* **2008**, *36*, 6434–6436. (In Chinese)
56. Til, F.K.; Yusunjiang, M.; Lin, L.; Reiner, D. Development of agricultural land and water use and its driving forces along the Aksu and Tarim River, P.R. China. *Environ. Earth Sci.* **2015**, *73*, 517–531. [[CrossRef](#)]
57. Qiu, J.Z.; Bo, J.F.; Li, D.C.; Wen, W.Z.; Qin, K.Y.; Guo, B.L.; Hubert, G. Dynamics and driving factors of agricultural landscape in the semiarid hilly area of the Loess Plateau, China. *Agric. Ecosyst. Environ.* **2004**, *103*, 535–543. [[CrossRef](#)]
58. Jiang, L.W.; Tong, Y.F.; Zhao, Z.J.; Li, T.H.; Liao, J.H. Water Resources, Land Exploration and Population Dynamics in Arid Areas—The Case of the Tarim River Basin in Xinjiang of China. *Popul. Environ.* **2005**, *26*, 471–503. [[CrossRef](#)]
59. Yu, Y.; Xiao, L.Z.; Jun, L.; Wei, D.; Wei, Y.Z.; Chao, G. Spatial integration of oasis city group around the western margins of the Tarim Basin. *J. Arid Land* **2010**, *2*, 214–221. [[CrossRef](#)]
60. Kennedy, J.J. From the tax-for-fee reform to the abolition of agricultural taxes: The impact on township governments in North-West China. *China Q.* **2007**, *189*, 43–59. [[CrossRef](#)]
61. Ito, J.; Ni, J. Capital deepening, land use policy, and self-sufficiency in China’s grain sector. *China Econ. Rev.* **2013**, *24*, 95–107. [[CrossRef](#)]
62. André, B.S. Introduction to spatial economic zones in China, illustrated by the Special Economic Development Zones of Horgos and Kashagr (Xinjiang Province). In *Jusletter*; Wiegand, W., Montani, S., Kummer, F., Eds.; Weblaw: Bern, Switzerland, 2014; p. 16.
63. Howard, K.W.F.; Howard, K.K. The new “Silk Road Economic Belt” as a threat to the sustainable management of Central Asia’s transboundary water resources. *Environ. Earth Sci.* **2016**, *75*, 976. [[CrossRef](#)]

